J|A|C|S
ARTICLES
Published on Web 08/17/2006

Transfer of Structural Elements from Compact to Extended States in Unsolvated Ubiquitin

Stormy L. Koeniger, Samuel I. Merenbloom, Sundarapandian Sevugarajan, and David E. Clemmer*

Contribution from the Department of Chemistry, Indiana University, Bloomington, Indiana 47405

Received April 10, 2006; E-mail: clemmer@indiana.edu

Abstract: Multidimensional ion mobility spectrometry techniques (IMS-IMS and IMS-IMS-IMS) combined with mass spectrometry are used to study structural transitions of ubiquitin ions in the gas phase. It is possible to select and activate narrow distributions of compact and partially folded conformation types and examine new distributions of structures that are formed. Different compact conformations unfold, producing a range of new partially folded states and three resolvable peaks associated with elongated conformers. Under gentle activation conditions, the final populations of the three elongated forms depend on the initial structures of the selected ions. This requires that some memory of the compact state (most likely secondary structure) is preserved along the unfolding pathway. Activation of selected, partially folded intermediates (formed from specific compact states) leads to elongated state populations that are consistent with the initial selected compact form—evidence that intermediates not only retain elements of initial structure but also are capable of transmitting structure to final states.

Introduction

Understanding how protein structures are established and evolve remains one of the most challenging problems of biochemistry.[1] While it is often possible to stabilize different structures in different environments, it is rarely possible to capture intermediates as the polypeptide chains fold or unfold. There remains substantial uncertainty about the number (and nature) of folding pathways, kinetics and timing associated with formation of structural elements, and the question of whether structural elements are intrinsic to the polypeptide chain or imposed by environmental factors. New ion sources[2] for mass spectrometry (MS) combined with labeling strategies make it possible to follow folding populations in a manner that complements other solution techniques.[3−5] An issue that arises in the study of conformations in the absence of solvation effects is the structure of the gas-phase ion.[6−21] For some systems, under some conditions, there is evidence that it may be possible to remove solvents in a manner that leaves an anhydrous form that retains a degree of memory of the solution state.[3,5−7,18,22,23]

In this paper, we use a new ion mobility spectrometry (IMS) instrument to select and activate ions having specific cross sections. We report transitions associated with activation of specific gas-phase conformation types of electrosprayed ubiq-

(1) Kuwajima, K. *Proteins: Struct., Funct. Genet.* **1989**, *6*, 87−103. Evans, P. A.; Radford, S. E. *Curr. Opin. Struct. Biol.* **1994**, *4*, 100−106. Bryngelson, J. D.; Onuchic, J. N.; Socci, N. D.; Wolynes, P. G *Proteins: Struct., Funct. Genet.* **1995**, *21*, 167−195. Dill, K. A.; Bromberg, S.; Yue, K. Z.; Fiebig, K. M.; Yee, D. P.; Thomas, P. D.; Chan, H. S. *Protein Sci.* **1995**, *4*, 561−602. Bryson, J. W.; Betz, S. F.; Lu, H. S.; Suich, D. J.; Zhou, H. X.; Oneil, K. T. Degrado, W. F. *Science* **1995**, *270*, 935−941.
(2) Karas, M.; Hillenkamp, F. *Anal. Chem.* **1988**, *60*, 2299. Tanaka, K.; Waki, H.; Ido, Y.; Akita, S.; Yoshida, Y.; Yoshida, T. *Rapid Commun. Mass Spectrom.* **1988**, *2*, 151−153. Fenn J. B.; Mann, M.; Meng, C. K.; Wong, S. F.; Whitehouse, C. M. *Science* **1989**, *246*, 64−71.
(3) Katta, A.; Chait, B. T. *J. Am. Chem. Soc.* **1993**, *115*, 6317−6321.
(4) Zhang, Z. Q.; Smith, D. L. *Protein Sci.* **1993**, *2*, 522−531.
(5) Miranker, A.; Robinson, C. V.; Radford, S. E.; Aplin, R. T.; Dobson, C. M. *Science* **1993**, *262*, 896−900. Hooke, S. D.; Eyles, S. J.; Miranker, A.; Radford, S. E.; Robinson, C. V.; Dobson, C. M. *J. Am. Chem. Soc.* **1995**, *117*, 7548−7549. Chung, E. W.; Nettleton, E. J.; Morgan, C. J.; Gross, M.; Miranker, A.; Radford, S. E.; Dobson, C. M.; Robinson, C. V. *Protein Sci.* **1997**, *6*, 1316−1324.
(6) Chowdhury, S. K.; Katta, V.; Chait, B. T. *J. Am. Chem. Soc.* **1990**, *112*, 9012−9013. Mirza, U. A.; Chait, B. T. *Int. J. Mass Spectrom. Ion Processes* **1997**, *162*, 173−181.
(7) Loo, J. A.; Loo, R. R. O.; Udseth, H. R.; Edmonds, C. G.; Smith, R. D. *Rapid Commun. Mass Spectrom.* **1991**, *5*, 101−105.
(8) Cheng, X.; Fenselau, C. C. *Int. J. Mass Spectrom. Ion Processes* **1992**, *122*, 109−119.
(9) Winger, B. E.; Light-Wahl, K. J.; Rockwood, A. L.; Smith, R. D. *J. Am. Chem. Soc.* **1992**, *114*, 5897−5899.
(10) Suckau, D.; Shi, Y.; Beu, S. C.; Senko, M. W.; Quinn, J. P.; Wampler, F. W.; McLafferty, F. W. *Proc. Natl. Acad. Sci. U.S.A.* **1993**, *90*, 790−793. Wood, T. D.; Chorush, R. A.; Wampler, F. M.; Little, D. P.; O'Connor, P. B.; McLafferty, F. W. *Proc. Natl. Acad. Sci. U.S.A.* **1995**, *92*, 2451−2454. McLafferty, F. W.; Guan, Z. Q.; Haupts, U.; Wood, T. D.; Kelleher, N. L. *J. Am. Chem. Soc.* **1998**, *120*, 4732−4740.
(11) Covey, T.; Douglas, D. J. *J. Am. Soc. Mass Spectrom.* **1993**, *4*, 616−623.
(12) Cox, K. A.; Julian, R. K., Jr.; Cooks, R. G.; Kaiser, R. E., Jr. *J. Am. Soc. Mass Spectrom.* **1994**, *5*, 127−136.
(13) Campbell, S.; Rodgers, M. T.; Marzluff, E. M.; Beauchamp, J. L. *J. Am. Chem. Soc.* **1994**, *116*, 9765−9766. Gard, E.; Green, M. K.; Bregar, J.; Lebrilla, C. B. *J. Am. Soc. Mass Spectrom.* **1994**, *5*, 623−631. Campbell, S.; Rodgers, M. T.; Marzluff, E. M.; Beauchamp, J. L. *J. Am. Chem. Soc.* **1995**, *117*, 12840−12854.
(14) Wolynes, P. G. *Proc. Natl. Acad. Sci. U.S.A.* **1995**, *92*, 2426−2427.
(15) Von Helden, G.; Wyttenbach, T.; Bowers, M. T. *Int. J. Mass Spectrom. Ion Processes* **1995**, *146*, 349−364. Wyttenbach, T.; von Helden, G.; Bowers, M. T. *J. Am. Chem. Soc.* **1996**, *118*, 8355−8364.
(16) Price, W. D.; Schnier, P. D.; Williams, E. R. *Anal. Chem.* **1996**, *68*, 859−866. Schnier, P. D.; Price, W. D.; Jockusch, R. A.; Williams, E. R. *J. Am. Chem. Soc.* **1996**, *118*, 7178−7189.
(17) Mesleh, M. F.; Hunter, J. M.; Shvartsburg, A. A.; Schatz, G. C.; Jarrold, M. F. *J. Phys Chem.* **1996**, *100*, 16082−16086. Shvartsburg, A. A.; Jarrold, M. F. *Chem. Phys. Lett.* **1996**, *261*, 86−91.
(18) Clemmer, D. E.; Jarrold, M. F. *J. Mass Spectrom.* **1997**, *32*, 577−592. Valentine, S. J.; Clemmer, D. E. *J. Am. Chem. Soc.* **1997**, *119*, 3558−3566. Valentine, S. J.; Anderson, J. G.; Ellington, A. D.; Clemmer, D. E. *J. Phys. Chem. B* **1997**, *101*, 3891−3900.

uitin. Ubiquitin is a small (76 residue) protein, and its structure and folding dynamics in solution have been the subject of extensive experimental and computational work.[24−27] More recently, studies involving the conformations of the gas-phase ions have been reported.[3,28−40] The results presented below indicate that activation of different compact forms (varying only slightly in cross section) of $[M + 7H]^{7+}$ ions (produced by electrospraying an acidic solution) can result in unfolding transitions that lead to substantially different final distributions of elongated structures. The results require that, during the unfolding transitions, some memory of the initial gas-phase compact structures is preserved in the intermediate and final states. As proposed previously,[41] we postulate that differences in final elongated forms are due to variation in secondary structure. This is the first study that provides direct evidence that populations of elongated conformations can retain a memory of initial structure after collisional activation.

The present work is closely related to several other studies of ubiquitin,[11,28,34,37,40] including some from our group.[30−32] Unsolvated ubiquitin ions favor three general types of structures: compact states, having cross sections $\Omega < 1120$ Å^2, partially folded states, where $1120 < \Omega < 1500$ Å^2, and elongated states, with $\Omega > 1500$ Å^2.[30] Additionally, the population of these states reflects the solution and electrospray conditions.[31] When compact states are stored in a Paul geometry ion trap,[32] they undergo unfolding transitions; although the ion temperature is not strictly known, three phenomenological transition threshold times (30, 575, and 1750 ms) for unfolding of the compact state can be observed—an indication of the existence of multiple structures (having the same initial cross section). Studies of structural transitions upon high-energy injection into drift tubes have also been performed;[30] however, these were done without selection of an initial state, and there was no evidence for differences in final distributions that would imply a memory of initial structures. The work presented below aids in our understanding of previous reports regarding ions in the gas phase, providing the first direct information about state-to-state pathways associated with transitions from different compact structures to different distributions of elongated structures. An understanding of the folding of polypeptide chains in the simplified gas-phase environment also complements general efforts to develop folding models.[42]

Experimental Section

Multidimensional Ion Mobility Measurements. The three drift region IMS-MS instrument used in these experiments is similar in design to instruments described elsewhere.[43−45] A schematic of the instrument is shown in Figure 1. A brief overview of the experimental sequence and instrumental parameters is as follows. Positively charged ions of ubiquitin (bovine, Sigma 90% purity) were formed by electrospraying a 3×10^{-5} M protein solution, 49:49:2 (% volume) water/acetonitrile/acetic acid, into the source region of an ion mobility/mass spectrometer. The continuous beam of ions is guided into an initial ion funnel (F1) similar to designs described by Smith and co-workers;[46] here, ions are radially focused along the axis of the drift tube and accumulated into a concentrated packet (for ~55 ms). The packet of ions is then released as a 100 μs pulse (by lowering the potential of a

(19) Zubarev, R. A.; Kelleher, N. L.; McLafferty, F. W. *J. Am. Chem. Soc.* **1998**, *120*, 3265−3266. Zubarev, R. A.; Kruger, N. A.; Fridriksson, E. K.; Lewis, M. A.; Horn, D. M.; Carpenter, B. K.; McLafferty, F. W. *J. Am. Chem. Soc.* **1999**, *121*, 2857−2862.

(20) Bernstein, S. L.; Liu, D. F.; Wyttenbach, T.; Bowers, M. T.; Lee, J. C.; Gray, H. B.; Winkler, J. R. *J. Am. Soc. Mass Spectrom.* **2004**, *15*, 1435−1443. Bernstein, S. L.; Wyttenbach, T.; Baumketnert, A.; Shea, J. E.; Bitan, G.; Teplow, D. B.; Bowers, M. T. *J. Am. Chem. Soc.* **2005**, *127*, 2075−2084.

(21) For general reviews, see: Miranker, A.; Robinson, C. V.; Radford, S. E.; Dobson, C. M. *FASEB J.* **1996**, *10*, 93−101. Bowers, M. T.; Marshall, A. G.; McLafferty, F. W. *J. Phys. Chem.* **1996**, *100*, 12897−12910. McLafferty, F. W.; Kelleher, N. L.; Begley, T. P.; Fridriksson, E. K.; Zubarev, R. A.; Horn, D. M. *Curr. Opin. Chem. Biol.* **1998**, *2*, 571−578. Hoaglund Hyzer, C. S.; Counterman, A. E.; Clemmer, D. E. *Chem. Rev.* **1999**, *99*, 3037−3079. Jarrold, M. F. *Acc. Chem. Res.* **1999**, *32*, 360−367. Jarrold, M. F. *Annu. Rev. Phys. Chem.* **2000**, *51*, 179−207. Konermann, L.; Simmons, D. A. *Mass Spectrom. Rev.* **2003**, *22*, 1−26. Hakansson, K.; Cooper, H. J.; Hudgins, R. R.; Nilsson, C. L. *Curr. Org. Chem.* **2003**, *7*, 1503−1525. Kelleher, N. L.; Hicks, L. M. *Curr. Opin. Chem. Biol.* **2005**, *9*, 424−430.

(22) Hudgins, R. R.; Woenckhaus, J.; Jarrold, M. F. *Int. J. Mass Spectrom.* **1997**, *165*, 497−507.

(23) Loo, J. A.; He, J. X.; Cody, W. L. *J. Am. Chem. Soc.* **1998**, *120*, 4542−4543.

(24) See, for example: Khorasanizadeh, S.; Peters, I. D.; Roder, H. *Nat. Struct. Biol.* **1996**, *3*, 193−205. Alonso, D. O. V.; Daggett, V. *Protein Sci.* **1998**, *7*, 860−874. Mayor, U.; Johnson, C. M.; Daggett, V.; Fersht, A. R. *Proc. Natl. Acad. Sci. U.S.A.* **2000**, *97*, 13518−13522. Colley, C. S.; Clark, I. P.; Griffiths-Jones, S. R.; George, M. W.; Searle, M. S. *Chem. Commun.* **2000**, *16*, 1493−1494. Krantz, B. A.; Moran, L. B.; Kentsis, A.; Sosnick, T. R. *Nat. Struct. Biol.* **2000**, *7*, 62−71. Krantz, B. A.; Sosnick, T. R. *Biochemistry* **2000**, *39*, 11696−11701. Jourdan, M.; Searle, M. S. *Biochemistry* **2001**, *40*, 10317−10325. Dastidar, S. G.; Mukhopadhyay, C. *Phys. Rev. E* **2003**, *68*, 021921. Marianayagam, N. J.; Jackson, S. E. *Biophys. Chem.* **2004**, *111*, 159−171. Sosnick, T. R.; Dothager, R. S.; Krantz, B. A. *Proc. Natl. Acad. Sci. U.S.A.* **2004**, *101*, 17377−17382. Zhang, J.; Qin, M.; Wang, W. *Proteins: Struct., Funct., Bioinf.* **2005**, *59*, 565−579. Jackson, S. E. *Org. Biomol. Chem.* **2006**, *4*, 1845−1853.

(25) See the following and references therein: Weber, P. L.; Brown, S. C.; Mueller, L. *Biochemistry* **1987**, *26*, 7282−7290. Monia, B. P.; Ecker, D. J.; Crooke, S. T. *Biotechnology* **1990**, *8*, 209−215. Harding, M. M.; Williams, D. H.; Woolfson, D. N. *Biochemistry* **1991**, *30*, 3120−3128. Briggs, M. S.; Roder, H. *Proc. Natl. Acad. Sci. U.S.A.* **1992**, *89*, 2017−2021. Khorasanizadeh, S.; Peters, I. D.; Roder, H. *Nat. Struct. Biol.* **1996**, *3*, 193−205. Pickart, C. M.; Eddins, M. J. *Biochim. Biophys. Acta* **2004**, *1695*, 55−72.

(26) Vijak-Kumar, S.; Bugg, C. E.; Cook, W. J. *J. Mol. Biol.* **1987**, *194*, 531−544.

(27) Brutscher, B.; Brüschweiler, R.; Ernst, R. R. *Biochemistry* **1997**, *36*, 13043−13053.

(28) Cassady, C. J.; Wronka, J.; Kruppa, G. H.; Laukien, F. H. *Rapid Commun. Mass Spectrom.* **1994**, *8*, 394−400. Cassady, C. J.; Carr, S. R. *J. Mass Spectrom.* **1996**, *31*, 247−254.

(29) Jockusch, R. A.; Schnier, P. D.; Price, W. D.; Strittmatter, E. F.; Demirev, P. A.; Williams, E. R. *Anal. Chem.* **1997**, *69*, 1119−1126.

(30) Valentine, S. J.; Counterman, A. E.; Clemmer, D. E. *J. Am. Soc. Mass Spectrom.* **1997**, *8*, 954−961.

(31) Li, J.; Taraszka, J. A.; Counterman, A. E.; Clemmer, D. E. *Int. J. Mass Spectrom.* **1999**, 37−47.

(32) Myung, S.; Badman, E.; Lee, Y. J.; Clemmer, D. E. *J. Phys. Chem. A* **2002**, *106*, 9976−9982.

(33) Badman, E.; Myung, S.; Clemmer, D. E. *Anal. Chem.* **2002**, *74*, 4889−4894. Badman, E. R.; Hoaglund-Hyzer, C. S.; Clemmer, D. E. *J. Am. Soc. Mass Spectrom.* **2002**, *13*, 719−723.

(34) Freitas, M. A.; Hendrickson, C. L.; Emmett, M. R.; Marshall, A. G. *Int. J. Mass Spectrom.* **1999**, *187*, 565−575.

(35) Reid, G. E.; Wu, J.; Chrisman, P. A.; Wells, J. M.; McLuckey, S. A. *Anal. Chem.* **2001**, *73*, 3274−3281.

(36) Zubarev, R. A.; Horn, D. M.; Fridriksson, E. K.; Kelleher, N. L.; Kruger, N. A.; Lewis, M. A.; Carpenter, B. K.; McLafferty, F. W. *Anal. Chem.* **2000**, *72*, 563−573. Breuker, K.; Oh, H. B.; Horn, D. M.; Cerda, B. A.; McLafferty, F. W. *J. Am. Chem. Soc.* **2002**, *124*, 6407−6420. Oh, H.; Breuker, K.; Sze, S. K.; Ge, Y. Carpenter, B. K.; McLafferty, F. W. *Proc. Natl. Acad. Sci. U.S.A.* **2002**, 15863−15868.

(37) Robinson, E. W.; Williams, E. R. *J. Am. Soc. Mass Spectrom.* **2005**, *16*, 1427−1437.

(38) Geller, O.; Lifshitz, C. *J. Phys. Chem. A* **2005**, *109*, 2217−2222.

(39) Pan, J. X.; Wilson, D. J.; Konermann, L *Biochemistry* **2005**, *44*, 8627−8633.

(40) Shvartsburg, A. A.; Fumin, L.; Tang, K.; Smith, R. D. *Anal. Chem.* **2006**, *78*, 3304−3315.

(41) Oh, H.; Breuker, K.; Sze, S. K.; Ge, Y.; Carpenter, B. K.; McLafferty, F. W. *Proc. Natl. Acad. Sci. U.S.A.* **2002**, *99*, 15863−15868.

(42) See the following and references therein: Popot, J. L.; Engelman, D. M. *Biochemistry* **1990**, *29*, 4031−4037. Sali, A.; Shakhnovich, E.; Karplus, M.; *Nature* **1994**, *369*, 248−251. Bryngelson, J. D.; Onuchic, J. N.; Socci, N. D.; Wolynes, P. G. *Proteins: Struct., Funct. Genet.* **1995**, *21*, 167−195. Dill, K. A.; Chan, H. S. *Nat. Struct. Biol.* **1997**, *4*, 10−19. Reich, L.; Weikl, T. R. *Proteins: Struct., Funct. Bioinf.* **2006**, *63*, 1052−1058.

(43) Koeniger, S. L.; Merenbloom, S. I.; Valentine, S. J.; Jarrold, M. F.; Udseth, R. D.; Smith, R. D.; Clemmer, D. E. *Anal. Chem.* **2006**, *78*, 4161−4174.

(44) Merenbloom, S. I.; Koeniger, S. L.; Valentine, S. J.; Plasencia, M. D.; Clemmer, D. E. *Anal. Chem.* **2006**, *78*, 2802−2809.

(45) Koeniger, S. L.; Merenbloom, S. I.; Clemmer, D. E. *J. Phys. Chem. B* **2006**, *110*, 7017−7021.

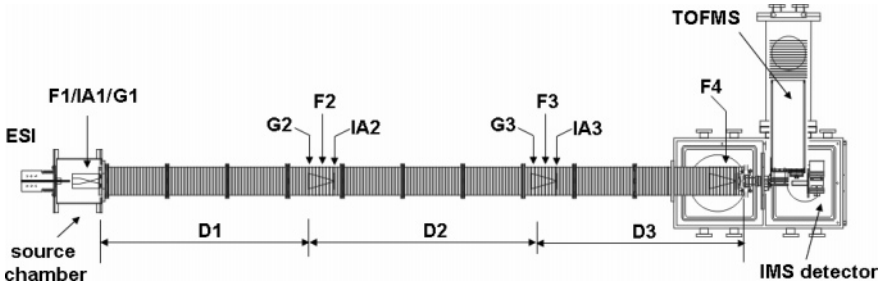

Figure 1. Schematic diagram of the experimental apparatus used for multidimensional ion mobility measurements. A combination of ion gates (G1−G3), ion funnels (F1−F4), and ion activation regions (IA1−IA3) are incorporated into the drift tube assembly. See text for details.

gating region, G1) into the first drift region (D1, ~94 cm long), and different charge states and structures separate under the influence of a uniform electric field (9 V·cm^{-1}) according to differences in mobilities. As mobility-dispersed ions exit D1, they pass through an ion gate region (G2) that can be operated such that all ions (or those only of a specified mobility) are allowed to enter a second drift region (D2). Ions exiting G2 enter a second ion funnel (F2) where they are radially focused,[43,47] and upon exiting F2 they enter an ion activation region (IA2). Thus, between the D1 and D2 regions, it is possible to select and activate a narrow distribution of ions, without significant loss of signal due to off-axis diffusion. The voltage across the activation region can be varied such that the transmitted ions undergo a range of energizing collisions with the buffer gas from essentially no activation (thermal conditions) to those that induce structural transitions without fragmenting the ions. At even higher energies, it is possible to induce fragmentation.[44] The ions transmitted through D2 are separated again until they enter a third ion gate (G3), funnel (F3), ion activation region (IA3), and drift region (D3, ~94 cm long). This region of ion selection and activation operates analogously to the G2/F2/IA2 region. Ions that exit the drift tube assembly are focused into a reflectron time-of-flight mass spectrometer.[48]

Selection and Activation of Narrow Distributions. Isolation of a narrow region of the distribution of mobility-separated ions is performed at the ion gates (G2 or G3). The ion gates of G2 and G3 are constructed with two grids spaced 0.30 cm apart with a delrin insulator[43] and function in a similar fashion as a Bradbury−Nielson gate. To select ions, the ion beam is deflected by raising a repulsive potential of 20 V to the second grid and then dropped for 100 μs to allow a short pulse of ions with a specified mobility to be transmitted into the drift region. The deflected ions are neutralized on the first grid. Timing of the ion gates is controlled by a pulse delay generator (model DG535, Stanford Research Systems, Inc.) and triggered by the initial pulse in the first ion funnel. Studies of voltages used to trap and gate ions indicate that there are no discernible changes in structure associated with handling of ions in either the source or gate regions.

To induce structural transitions (at IA2 and IA3), the ions are accelerated by changing the field. The IA2 and IA3 regions are ~0.3 cm long, and for the present studies we use activation voltages of 80−170 V. As ions accelerate through these regions, they gain energy through collisions with the buffer gas. Further collisions (immediately after the IA regions) cool the ions to the buffer gas temperature. This heating/cooling cycle to induce transitions is analogous to the variable injection energy approach pioneered by Jarrold and co-workers.[49]

Determination of Experimental Collision Cross Sections. It is useful to plot data on a cross-section scale. For drift tubes employing a uniform electric field, drift time distributions are converted to a cross-section scale using the relation[50]

$$\Omega = \frac{(18\pi)^{1/2}}{16}\frac{ze}{(k_bT)^{1/2}}\left[\frac{1}{m_I}+\frac{1}{m_B}\right]^{1/2}\frac{t_DE}{L}\frac{760}{P}\frac{T}{273.2}\frac{1}{N}$$

where z, e, k_b, m_I, and m_B correspond to the charge state, electron charge, Boltzmann's constant, and masses of the ion and buffer gases, respectively, and N is the neutral number density. The electric field strength (E), drift tube length (L), buffer gas pressure (P), and buffer gas temperature (T) are measured precisely, such that collision cross sections from any two measurements typically agree to within ±1% (relative uncertainty). The total drift times of ions in the present instrument are a composite of the time spent in each region, which is ultimately defined by the fields and trajectories (path length).

Although it is relatively straightforward to calibrate the drift time distributions for split-field instruments by using cross sections from the literature,[51] it is important to be able to determine reliable values directly from measurements within a single instrument. We have designed the D1 region such that, once ions enter this region, they experience a highly uniform field until they are selected at G2. In this case, the drift time of the selected ion corresponds to the delay time that is employed for selection in other regions,[43] ensuring a highly accurate measure of the mobilities of selected ions. We calibrate the drift times associated with the D2 + D3 and D3 regions in order to determine cross sections for new conformations that are formed upon activation.

Results and Discussion

Selection and Activation of Ions. Figure 2 shows several ion mobility distributions for the $[M + 7H]^{7+}$ state of electrosprayed ubiquitin that were recorded under different conditions. Included in this set is the initial distribution of ions formed by ESI. This spectrum shows that the distribution of $[M + 7H]^{7+}$ ions is dominated by compact states; the distribution is dominated by a sharp peak, centered at $\Omega \approx 1040$ Å^2, as well as a broad, unresolved shoulder associated with a distribution of lower-mobility ions that tails into the region defined as partially folded states. The total fraction of compact states sampled directly from ESI comprises ~80% of the distribution;

(46) Shaffer, S. A.; Tang, K. Q.; Anderson, G. A.; Prior, D. C.; Udseth, H. R.; Smith, R. D. *Rapid Commun. Mass Spectrom.* **1997**, *11*, 1813−1817. Shaffer, S. A.; Prior, D. C.; Anderson, G. A.; Udseth, H. R.; Smith, R. D. *Anal. Chem.* **1998**, *70*, 4111−4119. Shaffer, S. A.; Tolmachev, A.; Prior, D. C.; Anderson, G. A.; Udseth, H. R.; Smith, R. D. *Anal. Chem.* **1999**, *71*, 2957−2964. Kim, T.; Tolmachev, A. V.; Harkewicz, R.; Prior, D. C.; Anderson, G.; Udseth, H. R.; Smith, R. D.; Bailey, T. H.; Rakov, S.; Futrell, J. H. *Anal. Chem.* **2000**, *72*, 2247−2255.
(47) Tang, K.; Shvartsburg, A. A.; Lee, H. N.; Prior, D. C.; Buschbach, M. A.; Li, F. M.; Tolmachev, A. V.; Anderson, G. A.; Smith, R. D. *Anal. Chem.* **2005**, *77*, 3330−3339.
(48) Hoaglund, C. S.; Valentine, S. J.; Sporleder, C. R.; Reilly, J. P.; Clemmer, D. E. *Anal. Chem.* **1998**, *70*, 2236−2242.
(49) Jarrold, M. F.; Honea, E. C. *J. Am. Chem. Soc.* **1992**, *114*, 459−464. Hunter, J. M.; Fye, J. L.; Jarrold, M. F. *J. Chem. Phys.* **1993**, *99*, 1785−1795. Shelimov, K. B.; Jarrold, M. F. *J. Am. Chem. Soc.* **1996**, 118, 10313−10314.
(50) Mason, E. A.; McDaniel, E. W. *Transport Properties of Ions in Gases*; Wiley: New York, 1988.
(51) Myung, S.; Julian, R. R.; Nantia, S. C.; Cooks, R. G.; Clemmer, D. E. *J. Phys. Chem. B* **2004**, *108*, 6105−6111.

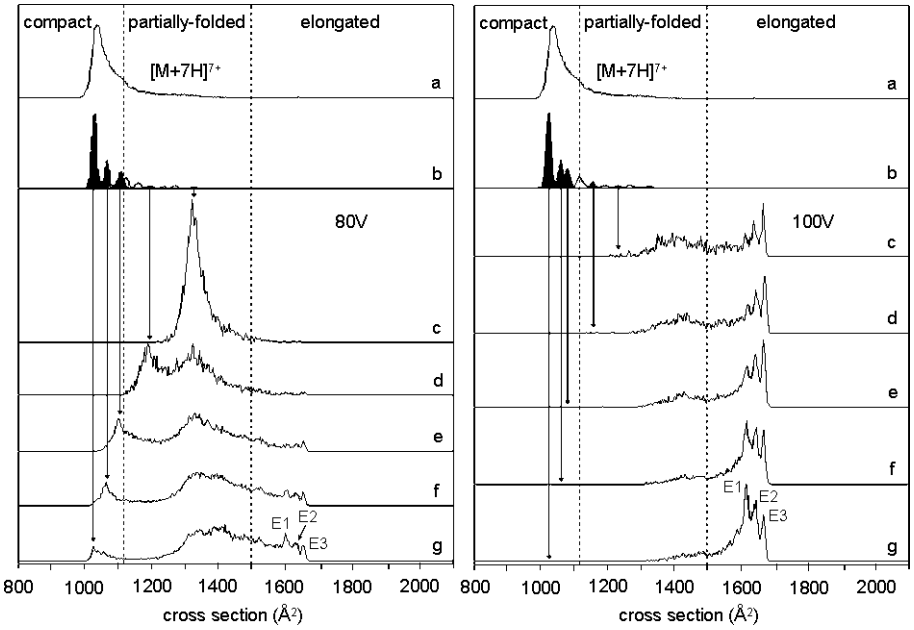

Figure 2. Ion mobility distributions of ubiquitin $[M + 7H]^{7+}$ ions, showing the initial distribution of ions formed by ESI (a) and nine narrow distributions of mobility-selected ions obtained by gating a 100 μs pulse of ions into D2 at various delay times (b). Activation of the selected ion distributions (shaded) at IA2 with a voltage of 80 V (left) and 100 V (right) produces distributions (c) through (g). The cross sections of the selected ions activated at 80 V were 1329 (c), 1196 (d), 1101 (e), 1063 (f), and 1025 Å^2 (g); and for 100 V were 1234 (c), 1158 (d), 1082 (e), 1063 (f), and 1025 Å^2 (g). The selection at 1063 Å^2 (shaded gray) shows a transition in the relative abundance of the three resolved elongated states (E1−E3) at 80 and 100 V. These distributions are obtained from nested $t_D(t_F)$ datasets by integration of a narrow range of m/z values for the $[M + 7H]^{7+}$ of ubiquitin. Dashed lines delineate the region in cross section for each conformer type. See text for discussion.

these conditions are consistent with our most gentle ion formation conditions and require that the level of collisional activation prior to additional experiments is minimal.

Application of the gating process (at G2, as described above) allows for ion selection; several narrow distributions of ions resulting from selection with no activation are shown in Figure 2. The observation that these distributions remain narrow over the remaining separation time is consistent with results that we have published recently.[45] The narrow peak shape requires that each narrow distribution of ion structures is relatively stable; that is, there appears to be no interconversion of one distribution of selected cross sections with another on the ~10−30 ms time scale of the experiment. If such interconversion between different compact states did occur, then selection of a narrow distribution would result in a broad peak and indicate the possibility of a distribution of structures that are in (or have begun the process of reaching) equilibrium. The sharp peaks that are observed upon selection in Figure 2 require that this is not the case. Rather, the sharp features that are selected from the original electrospray distribution of $[M + 7H]^{7+}$ ions must be a relatively narrow range of kinetically trapped structures, having cross sections that are so similar that, if unselected, they appear as a single broader, unresolved peak in the (i.e., the "all ions") ion mobility distribution shown in Figure 2a. Upon collisional or thermal activation (or storage in an ion trap) of the entire distribution of ions, only broad features associated with a range of partially folded and elongated ions are observed.[30−32]

Figure 2 also shows distributions that are obtained upon activation of several of the selected ions. Here, we consider two activation energies: 80 V (conditions we refer to as low-energy activation conditions) and 100 V (or high-energy activation conditions). Both conditions lead to changes in the distribution of the selected ions, indicating that structural transitions have occurred. Especially interesting is the observation that the new distribution that is formed depends on the position of the selected ions. For example, low-energy activation of the highest-mobility, compact ions produces a new distribution (Figure 2g) comprised of ~7% compact, ~65% partially folded, and 28% elongated structures, whereas activation of a narrow region of partially folded ions leads to formation of a broader distribution of partially folded states (Figure 2c,d).

It is interesting that, upon activation, the most compact ions are most efficient at producing extended states (especially relative to the partially folded forms). From considerations of the unfolding process, one expects partially folded ions (with greater cross sections) to be farther along on the unfolding pathway, and thus these might be expected to generate elongated states with highest efficiency. The present results indicate that this is not the case. Instead, it appears that the higher density of charge in the more compact form (i.e., the coulomb energy) is the impetus for generating the largest-cross-section forms of the extended states.[52,53] It is also interesting that no states appear to favor compact structures upon activation. This may indicate that compact forms of this charge state are less stable than the precursor states, or that the time required to produce compact ions (for example, from partially folded initial states) is much longer than the experimental time scale.

It is instructive to consider the distributions of the three resolved elongated structures (E1−E3) in more detail. These states can be favored under high-energy activation conditions. A striking feature of these data is that the populations of resolved

(52) Shelimov, K. B.; Clemmer, D. E.; Hudgins, R. R.; Jarrold, M. F. *J. Am. Chem. Soc.* **1997**, *119*, 2240−2248.
(53) Counterman, A. E.; Valentine, S. J.; Srebalus, C. A.; Henderson, S. C.; Hoaglund, C. S.; Clemmer, D. E. *J. Am. Soc. Mass Spectrom.* **1998**, *9*, 743−759.

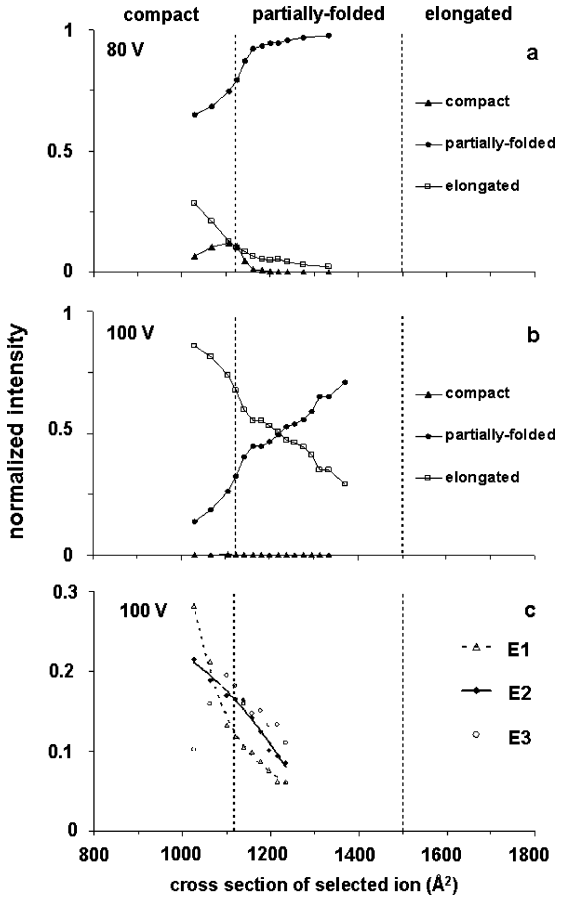

Figure 3. Relative populations of conformer types formed by activation of mobility-selected $[M + 7H]^{7+}$ ubiquitin ions as a function of the selected ion cross section. Populations represent the distributions shown in Figure 2 upon activation with 80 V (a) and 100 V (b). Relative populations of specific elongated structures (E1−E3) with respect to the total population are also shown (c). Dashed lines delineate the region in cross section for each conformer type.

elongated states clearly also depend on the initial structure that was selected for activation. We are surprised by this, because we have previously assumed any initial structure present to be randomized during the activation and unfolding process. Clearly this is not the case. Activation of the highest-mobility compact ions ($\Omega \approx 1025$ Å^2) leads to E1, E2, and E3 populations of ~28, ~21, and ~10%, respectively. In comparison, activation of selected lower-mobility compact forms (e.g., $\Omega \approx 1101$ Å^2) leads to populations of ~13, 17, and 20%, respectively. These differences are substantial; the fraction of E1 is a factor of ~2.2 greater when formed by activation of the high-mobility compact ions than when formed upon activation of lower-mobility compact states. In contrast, the population of E3 is a factor of 2 less (for these respective states).

Normalized Populations of States Formed upon Activation of Different Initial Structures. Figure 3 provides a plot of the relative populations (obtained by integrating appropriate regions of the normalized distributions for all of the data we have recorded) of the compact, partially folded, and elongated conformer types formed upon activation as a function of the cross section of the selected ion. Under low-energy activation conditions, high-mobility compact ions give rise to all three conformer types (i.e., compact, partially folded, and elongated) upon activation. As the selected ion cross section of the compact state is increased to values near the partially folded threshold, the fraction of remaining compact states that is produced increases, apparently at the expense of formation of elongated states (which shows a decrease in population). For this region, there is a slight increase in the partially folded states. Thus, it appears that the highest-mobility compact forms are most capable of producing elongated states (at low energies). This is again consistent with the notion that these compact structures may be relatively destabilized by coulomb interactions.

At higher energies, the populations of partially folded and elongated states formed upon activation appear to be in direct competition; each varies with a nearly linear dependence on the cross section of the initial selected state. Elongated structures are favored upon activation of compact precursors, whereas partially folded states are favored upon activation of partially folded precursors (i.e., $\Omega \geq 1215$ Å^2).

Figure 3 also shows the populations for the E1, E2, and E3 states (obtained upon activation at 100 V). The transition in abundance between these three states is observed within the compact conformer type at $\Omega \approx 1065$ Å^2. Prior to this transition, E1 is most abundant and E3 is least abundant. E3 dominates the elongated distributions for activation of low-mobility compact and partially folded initial states.

Evidence for a Memory of Initial Structure in the Final State. Taken in total, the variations in final populations that are observed upon activation of specific distributions of ions require that the latter forms have retained some degree of memory of the structures of the initial states. For example, by examining the ratios of E1 and E3 in Figure 3, it is possible to determine which compact states were the precursors. The observation of an E1 population greater than that of E3 indicates a high-mobility compact form, whereas a population of E3 > E1 indicates lower-mobility compact states.

A substantial amount of work involving the characterization of ubiquitin structures in solution has been reported.[24−27] Under native solution conditions, the protein exists as a compact, tightly folded structure that incorporates a β-sheet and two α-helical regions.[26] In high-acidity solutions (similar to the solution used for ESI), ubiquitin favors an A state that conserves the secondary structure associated with the α-helical regions of the N-terminal half of the protein; the β-sheet character associated with the C-terminal half is largely converted to a helix.[27] To have a cross section in excess of ~1600 Å^2, ubiquitin must exist as a highly extended structure that retains little or no elements of the tertiary folds found in solution; from these arguments, the memory of initial conformation that is preserved in the final distribution of elongated states must arise from differences in secondary structure that are preserved after unfolding of the initial compact states. Consistent with these ideas, McLafferty and co-workers have examined ubiquitin ions by electron capture dissociation and found evidence for substantial secondary structure in the absence of solvent.[36,41]

Is Structural Information from Initial States Preserved and Transferred through Partially Folded Intermediates? An important question that arises in these studies is how is the memory of the structure of the compact state transferred into the final distribution of elongated conformations. For example, does a compact conformation sample a partially folded structure prior to forming an elongated state, or does the compact to elongated transition avoid partially folded states (where the memory of the initial conformation may be lost)? To address

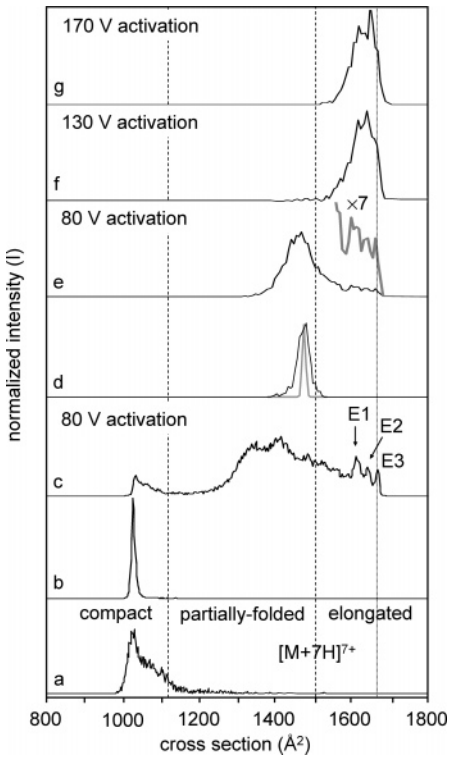

Figure 4. Ion mobility distributions of ubiquitin $[M + 7H]^{7+}$ ions obtained in IMS-IMS-IMS/MS experiments. Distribution **a** is the initial distribution consisting of primarily compact conformers. Upon selection of a narrow distribution of compact ions at G2 (100 μs), distribution **b** is obtained. Activation of the selected compact ions at IA2 produces distribution **c**. A second selection of an intermediate within the partially folded structures performed at G3 (150 μs) is shown in **d**, with the diffusion-limited peak width of the selected ion (gray line). Upon activation of the partially folded structures at IA3, distribution **e** is produced, consisting of a broader distribution of partially folded structures and a smaller distribution of elongated states (gray line). Distributions **f** and **g** are obtained upon higher-energy activation of the partially folded structures shown in **d**. These distributions are obtained from nested $t_D(t_F)$ datasets by integration of a narrow range of m/z values for the $[M + 7H]^{7+}$ of ubiquitin. See text for discussion.

these issues, consider the data in Figure 4. Here, the selected high-mobility compact structures ($\Omega \approx 1025$ Å^2) are activated under low-energy conditions to produce a new distribution of states: ~6% compact, ~65% partially folded, and ~29% elongated structures. From this new distribution, a narrow distribution of intermediate structures within the partially folded conformer type is selected at $\Omega \approx 1485$ Å^2, and these ions are exposed to low-energy activation. Several features of this selection are noteworthy. Unlike selections (such as the sharp feature in Figure 4b) from the initial distribution (Figure 4a), selections of these intermediate states (produced upon activation, Figure 4c) do not appear to be as stable.[45] That is, during the final separation (through D3), the peak associated with the partially folded selected ions (Figure 4d) broadens—an indication that the region that was selected samples other conformations during the time required for transmission through D3. For comparison, we show the diffusion-limited peak shape calculated from the transport equation.[50] A comparison of the full widths at half-maxima of the experimental and theoretical peaks shows that the former is a factor of ~3 broader, indicating that a range of partially folded states are sampled on the experimental time scale. Additionally, low-intensity shoulders (on both sides of the peak) are observable.

Upon low-energy activation, the selected partially folded states ($\Omega \approx 1485$ Å^2) broaden even more (Figure 4e). It appears that some more compact, partially folded ions are formed ($\Omega < 1485$ Å^2), as well as some partially folded structures that have more open conformations ($\Omega > 1485$ Å^2). Additionally, a small population of elongated ions is produced. These ions have mobilities that are consistent with the E1, E2, and E3 states; integration of the areas under each feature yields relative populations of 47, 27, and 21%. That is, the population of E1 is a factor of ~2.2 greater than the population of E3, the same ratio observed for elongated structures formed directly upon activation of the high-mobility compact structures (Figure 2). Thus, we conclude that the $\Omega \approx 1485$ Å^2 intermediates formed from the high-mobility compact ions can also preserve the ratios of E1, E2, and E3 states that were observed in Figure 3.

At higher activation energies (130 and 170 V, also shown in Figure 4), it is possible to convert all of the partially folded selected ($\Omega \approx 1485$ Å^2) ions into elongated conformations; however, the peak shape broadens. Under both of these higher activation conditions, a new reproducible feature that is not well resolved ($\Omega \approx 1650$ Å^2) is the largest peak in the distributions. This new unresolved distribution (observed at higher activation energies) appears to have lost much of the memory associated with lower energy activation.

Summary and Conclusion

IMS-IMS/MS and IMS-IMS-IMS/MS techniques have been used to select and activate narrow distributions of conformation of the ubiquitin $[M + 7H]^{7+}$ state formed by ESI. The final distributions of states that are observed are highly dependent upon the initial distribution of selected ions. At low activation energies (80 V), compact states unfold to form a broad distribution of partially unfolded states as well as a smaller distribution of elongated structures. We note that this is the first observation of three resolved peaks associated with the elongated structure. Low-energy activation of narrow distributions of partially folded states leads to a broader distribution of ions still within the range associated with partially folded states. At high energy (100 V), it is possible to observe the three resolved peaks associated with extended structures.

It is interesting to consider the implications of the present results. First, it is clear that the population of the resolved unfolded states (E1−E3, Figures 2−4) depends on the initial distribution that is selected for activation. Activation of the highest-mobility form within the compact state to produce elongated ions favors formation of E1 elongated states (at low and high activation energies), whereas activation of a low-mobility distribution of compact ions favors E3. The observation that the distribution of elongated structures that is produced upon activation depends on the initial structure that is selected requires that the final distribution of elongated conformers has a memory of the initial state that was selected for activation.

In other IMS-IMS-IMS/MS studies, selection and activation of an intermediate (partially folded distribution) formed upon activation of an initial high-mobility compact state leads to primarily partially folded structures, with a small population of the resolved elongated states (E1−E3). The distribution of final elongated states (originating from the selected partially folded intermediate) resembles the population of elongated structures formed directly from the high-mobility compact initial structure.

Thus, it appears that the partially folded intermediate not only retains a memory of the initial high-mobility state but also can transmit the distribution to the final distribution of elongated structures.

With these ideas in mind, it is interesting to consider the nature of structure that might be preserved. In previous studies, we have noted that the cross sections of elongated ions are much larger than the calculated values for folded structures, such as structures obtained from crystallographic and solution nuclear magnetic resonance studies; we anticipate little or no remaining tertiary structure. Instead, we postulate that elongated conformations may differ in the level of secondary structure that is preserved through the activation process. While this conclusion requires further investigation, it is supported by studies of secondary structure by MS-based techniques.[41] Overall, one might speculate that loss of tertiary structure through low-energy collisions may not impede the ability of recently developed nonergodic dissociation methods[19,36,41,54−57] to examine secondary structure.

Acknowledgment. We are grateful to Evan Williams, Fred McLafferty, and Dick Smith for sharing several studies of the structures of gas-phase ubiquitin prior to publication. This work is supported in part by grants from the National Science Foundation (CHE-0078737), the National Institutes of Health (AG-024547-01 and P41-RR018942), the Indiana 21st Century fund, and the Analytical node of the Indiana University METACyt Initiative (funded by a grant from the Lilly Endowment).

JA062137G

(54) Adams, C. M.; Kjeldsen, F.; Zubarev, R. A.; Budnik, B. A.; Haselmann, K. F. *J. Am. Soc. Mass Spectrom.* **2004**, *15*, 1087−1098.
(55) Syka, J. E. P.; Coon, J. J.; Schroeder, M. J.; Shabanowitz, J.; Hunt, D. F. *Proc. Natl. Acad. Sci. U.S.A.* **2004**, *101*, 9528−9533.
(56) Pitteri, S. J.; Chrisman, P. A.; Hogan, J. M.; McLuckey, S. A. *Anal. Chem.* **2005**, *77*, 1831−1839. Hogan, J. M.; Pitteri, S. J.; Chrisman, P. A.; McLuckey, S. A. *J. Proteome Res.* **2005**, *4*, 628−632.
(57) Devakumar, A.; Thompson, M. S.; Reilly, J. P. *Rapid Commun. Mass Spectrom.* **2005**, *19*, 2313−2320.